Using Electroless Deposition for the Preparation of Micron Sized Polymer/Metal Core/Shell Particles and Hollow Metal Spheres

Pietro Tierno[†] and Werner A. Goedel*[,†,‡,§]

Organic and Macromolecular Chemistry, OCIII and Materials & Catalysis, ACII, University of Ulm, and Department of Physical Chemistry, Chemnitz University of Technology

Received: July 29, 2005; In Final Form: November 17, 2005

Uniform and stable core-shell microspheres composed of a poly(methyl methacrylate) (PMMA) core and a thin metallic shell of nickel−phosphorus, cobalt−phosphorus, or mixed metal alloys (CoNiP, NiFeP, CoFeP) were prepared by dispersion polymerization of methyl methacrylate followed by electroless plating. The presence of the metallic shell around the particles was confirmed by scanning electron microscopy, energy-dispersive X-ray spectroscopy, and photoelectron spectroscopy. Transmission electron microscopy images of the cross-section of individual particles show that the thickness of the metal/alloy can be precisely tuned by adjusting the immersion time of the microspheres in the electroless bath. Depending on the deposited metallic material, various magnetic properties, from paramagnetic to ferromagnetic, are achieved. Finally, uniform hollow metallic spheres composed of nickel, cobalt, or nickel−cobalt alloy are obtained by dissolving the polymer core.

I. Introduction

Spherical particles are convenient and often used as model systems for studying ensembles of mutually interacting bodies[1] or as "handles" attached to an object of interest.[2] Especially advantageous is the use of optical tweezers[3] or magnetic tweezers[4] to manipulate individual dielectric or magnetic spheres. On the other hand the mutual interaction between dielectric or magnetic spheres in ensembles can easily be manipulated by external electric or magnetic fields. In these investigations it is always necessary to tailor the size of the particles to the method and phenomena under consideration. Submicroscopic spheres have the advantage that one can neglect gravity and that they have a less disturbing effect on their surrounding. Large spheres, on the other hand, have the advantage that they are visible[5] and thus can be easily monitored by optical methods. Furthermore, the size of particles significantly influences the strength of interaction with external fields or with neighboring particles.

While there is a significant knowledge on the preparation of magnetic particles of diameters of either a few hundred nanometers[6] or dozens of microns,[7] there is an obvious lack of synthetic methods for the preparation of micron-sized spheres having tunable magnetization with a paramagnetic or even ferromagnetic behavior. In recent years, new techniques have been proposed to synthesize composite microspheres made by an organic core and inorganic shell[8] or vice versa.[9] Especially, combining a core of organic polymers with a metallic shell yields particles of low average density, electrical conductivity, and magnetic or even ferromagnetic behavior.[10−12] Such particles can be prepared by the coating of preformed organic spheres via electroless deposition. In this technique the polymeric spheres are first decorated with Pd seed particles and then immersed in an appropriate solution of metal salts and reducing agents. The current literature describes magnetic core/shell particles prepared this way, almost exclusively based on nickel coating.[13−15]

Pure nickel has ferromagnetic properties. On the other hand, coating the particles with other alloys such as Co, Co−Ni, Co−Fe offers the advantage of tailoring their magnetic properties from paramagnetic to ferromagnetic. Using this concept, we have synthesized various micron-sized particles coated by several metal alloys (NiP, CoP, NiFeP, CoNiP, CoFeP) via electroless deposition. Here, we describe the preparation of these particles and their characterization.

II. Experimental Section

Particle Synthesis. Monodisperse poly(methyl methacrylate) (PMMA) particles having a mean radius of 4.04 μm and a density of 1.19 g/cm^3 were synthesized by dispersion polymerization.[16] In a typical reaction 0.6 g (0.4% by w.) of 2,2′-azobis(2-methylpropionitrile) (AIBN, Acros Organics) (recrystallized from absolute ethanol) were mixed with 6 g (4.0% by w.) of poly(vinyl pyrrolidone) (PVP40 K-30, MW = 40.000, Sigma Aldrich) and 100 mL of absolute methanol and finally 10.6 mL of methyl methacrylate (MMA, Merck) (washed first with a 10% aqueous sodium hydroxide solution, subsequently with deionized water until neutral and finally passed through aluminum oxide). The reaction mixture was degassed by several freeze/pump cycles, warmed by immersing it into a temperature-controlled bath that was heated from room temperature up to 55 °C at a rate of 1 °C/min and then kept at this temperature for 48 h. The reaction vessel was filled with N_2 atmosphere and stirred at a rate of ∼40 rpm, starting after the last thawing step. The freshly synthesized particles were washed and redispersed in highly deionized water (from Milli-Q system, Millipore) using four centrifugation and redispersion cycles.

* Corresponding author: Werner A. Goedel, Chemnitz, University of Technology, Physical Chemistry, Strasse der Nationen 62, 09111 Chemnitz (Germany) Tel: +49 371-531 1713. E-mail: werner.goedel@chemie.tu-chemnitz.de

† Organic and Macromolecular Chemistry, University of Ulm.

‡ Materials & Catalysis, Universit of Ulm.

§ Chemnitz University of Technology.

10.1021/jp054213s CCC: $33.50
Published on Web 02/16/2006

TABLE 1: Bath Composition and Operating Conditions for the Electroless Plating[a]

	Process					
	NiP1[17a]	NiP2[17a]	CoP[17b]	CoNiP[17c]	CoFeP[17d]	NiFeP[17d]
	Compounds [mol/dm^3]					
$NiSO_4 \cdot 6H_2O$	0.11	0.08		0.05		0.01
$CoSO_4 \cdot 7H_2O$			0.06	0.03	0.09	
$FeSO_4 \cdot 7H_2O$					0.07	0.07
$NaH_2PO_2 \cdot H_2O$	0.17	0.20	0.23	0.23	0.48	0.48
$Na_3C_6H_5O_7 \cdot 2H_2O$[b]	0.20	0.14	0.12		0.20	0.20
NH_4Cl	1.10					
$(NH_4)_2SO_4$			0.50	0.25	0.10	0.10
	Conditions					
pH	10.0	9.0	7.8	7.8	10	10
temperature (°C)	60−65	65	60−65	60−65	65−70	65−70
	Molar ratio					
Ni:Co:Fe:P	39.2:0:0:60.8	28.6:0:0:71.4	0:20.7:0:79.3	16.1:9.7:0:74.2	0:14.1:10.9:75.0	1.8:0:12.5:85.7

[a] All quantities are given in mol/L. The baths were modified versions of ref 17, as indicated in the table. [b] Trisodiumcitrate dihydrate.

Activation. First the particles were dispersed in a mixture of 5 mL of concentrated HCl and 95 mL of water for ∼3 min, separated from this solution by centrifugation and redispersed in deionized water. This dispersion was shaken for ∼3 min and the particles were isolated again via centrifugation. 5 g of the wet particles were dispersed in ∼130 mL of a solution containing 10 g/L of $SnCl_2$ + 5 mL/L HCl, were isolated by centrifugation, washed as described above, and then redispersed in ∼130 mL of a solution containing 0.5 g/L of $PdCl_2$ + 4 mL/L HCl. After these operations, the particles changed color and became brown due to the presence of Pd on their surface.

Electroless Plating. The particles were separated, washed again, and directly used for the electroless plating. The particles were redispersed in the plating solution contained in a Pyrex glass beaker mounted in a temperature-regulated water bath and equipped with a mechanical stirrer and a nitrogen bubbling system. The baths used were variations of plating baths described in the literature.[17] Details on their composition, pH, and temperature are given in Table 1. After plating, the coated microspheres were washed twice, dried under nitrogen atmosphere, and finally annealed in a vacuum oven at 120 °C for ∼12 h. To avoid oxidation of the metallic surface, the particles were redispersed and stored in pure methanol that was deoxygenated by passing a stream of Argon through it.

Hollow Spheres. The coated microspheres were redispersed in toluene for ∼12 h, then annealed at 120 °C and redispersed as described above for the coated spheres.

Particle Characterization. The morphology and the composition of the coated microspheres were analyzed using a scanning electron microscope (SEM, DSM 962, Zeiss Germany) equipped with an energy-dispersive X-ray spectrometer (EDAX). To prevent surface charging, the samples were covered for SEM with a 20 nm thin layer of Au−Pd (the addition of Pd to the gold gives rise to a small grain size), while for the EDAX spectra a thin carbon film of ∼2 nm was applied (has minimal interference with the detection of heavier elements). For imaging their cross-section, the particles were embedded in epoxy resin (Epofix Struers, Denmark), polished, cut with a LKB ultramicrotome (Ultratone NOVA, LKB 2188, Bromma, Sweden), and finally imaged with a transmission electron microscope (TEM, EM400T Philips, Netherlands). For TEM of whole particles, the particles were placed on carbon-covered electron microscopy grids (Plano Co., Germany).

The magnetic measurements of dilute suspensions of the particles in water were performed at $T = 300$ K using a Vibrating Sample Magnetometer (VSM, Lake Shore Cryotronics, 7300/9300 series). Before the measurements, a suspension of the particles (∼1% w.) was loaded into a quartz glass tube and placed inside a specially designed plate mounted inside the VSM.

Thermogravimetric analysis of the dry particles (TGA/SDTA851[e] from Mettler Toledo, Germany) was performed in nitrogen atmosphere using a heating rate of 10 °C/min.

The crystalline structure of the coating was determined using a STOE IPDS X-ray diffractometer operating with Cu Kα radiation.

X-ray photoelectron spectroscopy was made by using a PHI 5800 ESCA system (Physical Electronics) with monochromatized AlKα (250.0 W, 187.85 eV) and MgKα X-ray (350.0 W, 187.85 eV) radiations as the excitation source.

A public domain image processing program (Image J,[18]) was employed to analyze the SEM and TEM images of the PMMA microspheres and to obtain their average diameter and particle size distribution.

Calculation of the Shell Thickness from Thermogravimetric Analysis. Thermogravimetric analysis of the particles gives the relative weight loss. This quantity, ω, can be related to the mass of the particles as

$$\omega = \frac{m_{\text{shell}}}{m_{\text{shell}} + m_{\text{core}}} \leftrightarrow \frac{m_{\text{core}}}{m_{\text{shell}}} = \frac{1}{\omega} - 1$$

where $m_{\text{shell}} = V_{\text{shell}} \cdot \rho_{\text{shell}}$ is the mass of the metallic layer of thickness δ on the microsphere, with a volume $V_{\text{shell}} = (4/3)\pi((R + \delta)^3 - R^3)$ and a density ρ_{shell}; $m_{\text{core}} = V_{\text{core}} \cdot \rho_{\text{core}}$ is the mass of the pristine particles with volume $V_{\text{core}} = (4/3)\pi R^3$ and density ρ_{core}. The mass ratio can be rewritten in terms of the volumes as

$$\frac{m_{\text{core}}}{m_{\text{shell}}} = \frac{\rho_{\text{core}} V_{\text{core}}}{\rho_{\text{shell}} V_{\text{shell}}} = \frac{\rho_{\text{core}}}{\rho_{\text{shell}}} \frac{1}{(1 + \delta/R)^3 - 1}$$

to finally yield

$$\delta = R\left(\sqrt[3]{\left(\frac{\rho_{\text{shell}}}{\rho_{\text{core}}}\right) \cdot \left(\frac{\omega}{1 - \omega}\right) + 1} - 1\right)$$

The density of the pristine particles is known (1.19 g/cm^3), while the density of the deposited metal can be approximately estimated from the knowledge of the fraction of the elemental composition (obtained from the EDAX analysis) and the density

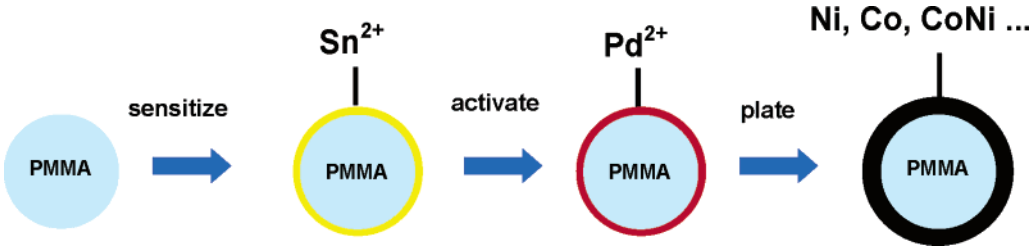

Figure 1. Schematic representation of the general procedure used to prepare polymer microspheres coated with a metallic shell.

of the corresponding material. For example, for a NiP alloy the density was approximated to be given by

$$\rho_{NiP} = x_{Ni}\,\rho_{Ni} + x_P\,\rho_P$$

where x is the fraction of the material present (x_{Ni} refer of nickel, x_P to phosphorus etc.).

Magnetic Properties. The magnetic properties of the coated microspheres were obtained by first measuring the magnetization loop of the pristine polymer particles used as core. Fitting this curve with a straight line, we calculate the diamagnetic susceptibility of the particles as: $\chi_{dia} = -1.82 \times 10^{-7} \pm 0.08 \times 10^{-7}$ and then, to obtain the pure magnetic contribution of the microspheres, we rescale all the magnetization graphs using χ_{dia}:

$$M(H) = M(H)_{measured} - \chi_{dia}H$$

The data were then normalized with respect to the weight of the dry sample of particles. Because we found a paramagnetic behavior for some samples, we perform a Langevin fit of the magnetization curves using the expression

$$M(H) = M_s\left(\coth\left(\frac{\mu_0 mH}{k_B T}\right) - \frac{k_B T}{\mu_0 mH}\right)$$

were M_s is the saturation magnetization, k_B the Boltzmann constant, $T = 300$ K, and m the magnetic moment (we express m in terms of the Bohr magneton $\mu_B = 9.27 \times 10^{-24}$ Am^2).

III. Results and Discussion

The aim of this work was the preparation of composite microspheres made by a polymer core and a metallic shell with tunable magnetic properties.

The general procedure used to produce these particles is schematically depicted in Figure 1. First monodisperse poly(methyl methacrylate) (PMMA) microspheres were synthesized by dispersion polymerization (a picture showing an overview of the resulting particles and their size distribution can be found in the Supporting Information). For the deposition process we choose to use as core polymer particles instead of inorganic particles (e.g., silica or glass) because of their lower density (1.19 g/cm^3 vs. 2.0 g/cm^3 for silica), and because they are more easily prepared with a narrow size distribution.

To deposit the metal on the nonconductive surface of these particles, a catalytic activation before the metallization process was necessary. We follow the 2-step method in which the particles are first "sensitized" by absorption of Sn^{2+} nuclei, and then "activated" by further absorption/deposition of Pd^{2+} nuclei on their surface.[19] We prefer this activation procedure to the more common "one step" method (that uses a mixed Sn−Pd solution) due to the better adhesion of the catalytic sites.[20] After the activation procedure the microspheres were immersed in an electroless plating bath and thus metalized.

Compared to galvanic deposition (e.g., electroplating), electroless plating allows to deposit a uniform metal film on nonconductive surfaces (for example polymers) and does not require any external electrical potential.[20] However, it is more difficult to control due to the significant influence of various variables (composition of the bath, pH, temperature, preprocessing, etc.) on the stability of the process and, consequently, on the uniformity of the plating. Therefore, the target of our first experiments was to find the optimal bath composition and then to determine the growth rate of these films.

Figure 2 displays the results of plating microspheres with nickel−phosphorus alloy (NiP) using increasing reaction time. From top to the bottom (Figure 2b to Figure 2d) the reaction time was increased. Figure 2a shows the pristine polymer particles without any metallic layer. Figures 2b−2d show the same particles but coated with layers of a nickel−phosphorus alloy with low phosphorus content (NiP1, Table 1). The thickness of the nickel layer was increased by prolongation of the immersion time of the particles in the electroless bath. This increase in shell thickness is even better visible in the TEM images 2f to 2h that show the cross-sections of coated particles. Figure 2e shows the thickness of the metallic layer obtained as a function of the plating time (black square). In addition, we subjected the coated particles to thermogravimetric analysis (see Figure 5d for representative examples) and inferred the layer thickness from the weight loss of the coated particles in the temperature range of 100° to 400°. The corresponding data are included in Figure 2e (red circle) and show a similar trend as the TEM measurements.

Comparing the first SEM image with the others it is obvious that there is a metal deposit on the polymer particles of higher roughness than the pristine surface. Regarding the morphology of the deposited alloy, the nickel film was quite uniform after 10 min of plating (~0.23 μm thickness), while a more granular structure started to appear for immersion times exceeding 10 min. The TEM images (Figures 2f−h) confirm this change in the particle morphology and also show that after 20 min of coating some cracks start to appear in the metallic shell. The presence of these breaches in the metallic shell was mainly due to the development of internal stress related to the low phosphorus content of the deposit.[21] They furthermore reveal that the shell thickness increases with increasing the immersion time. This can be seen again if the shell thickness (obtained from TEM as well as obtained from the residual mass in TGA) is plotted versus the immersion time in Figure 2e. Compared to the TEM analysis, the TGA measurements reveal a higher thickness. This deviation was due to the fact that TGA analysis includes excess metal alloy not sticking to the particles, while TEM was performed only on core−shell particles that were cut perpendicular through their center.

Using electroless plating to coat the particles gives the additional advantage of tailoring the nature of the plated alloy by simply changing the components of the plating bath and,

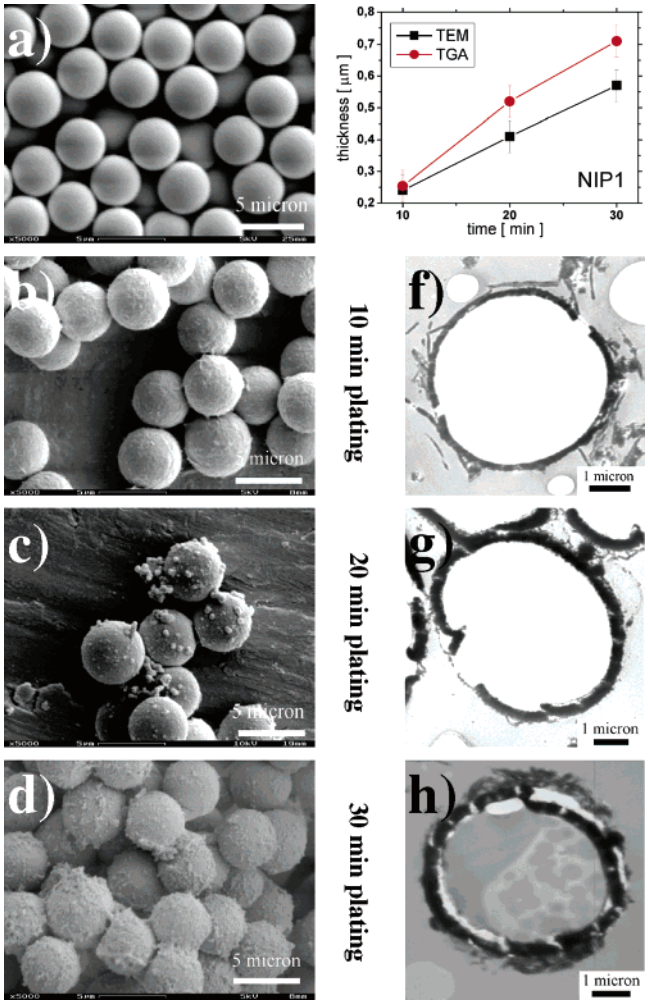

Figure 2. Series of SEM images showing: (a) PMMA particles used as core, (b) PMMA particles coated with a NiP layer (low P coating, bath of Table 1), obtained after 10 min of immersion times in the plating bath; (c) after 20 min; (d) after 30 min; (e) diagram of the metallic thickness as function of the plating time (black squares: thickness obtained from TEM images; red circles: thickness calculated from TGA measurements); (f−h) corresponding TEM images of cross-sections of the particles.

when necessary, its operating conditions (see Table 1). A proper combination of these alloys may allow us to prepare microspheres with completely different magnetic behavior. For example the inclusion of a strong ferromagnetic material such as cobalt, alone or together with the nickel, can enhance the magnetic properties of the microspheres. On the other hand, one can weaken the magnetic properties of the particles even down to a paramagnetic character by including increasing amounts of a non metallic component such as phosphorus. In this context, we have performed a second series of experiments in which we used several baths to deposit various alloys on the particles. The main results of these experiments are displayed in Figure 3. For brevity we will call the deposited alloys as: NiP1 = nickel with low phosphorus content (already shown in Figure 2), NiP2 = nickel with high phosphorus content, CoP = cobalt−phosphorus, CoNiP = cobalt−nickel−phosphorus, NiFeP = nickel−iron−phosphorus, and CoFeP = cobalt−iron−phosphorus. All the images and graphs of Figure 3 are grouped in six rows, each row corresponds to a different alloy (in order, NiP1, NiP2, CoP, CoNiP, NiFeP, and CoFeP). Each of the rows contains a SEM picture of the coated microspheres, a TEM image of the cross-section of an individual microsphere (in the second row the PMMA core was depolymerized by the electron beam in the microscope), the EDAX spectrum, and the magnetization curve. All the images and diagrams refer to microspheres coated by 10 min of plating (a diagram that shows the thickness of the metallic layers in function of the plating time for all the alloys is shown in the Supporting Information).

The electron microscopy images show that it was possible to deposit various metallic alloys onto the polymer particles. The NiP1 was the most uniform while the CoNiP, CoFeP, and the NiFeP alloys present a more granular structure. In agreement with this observation, we note that non uniform deposition of these alloys was previously reported in the literature.[22]

To estimate the elemental composition of the coatings, we performed EDAX and XPS analysis of the coated microspheres (for quantitative data see Table 2, detailed EDAX-diagrams are integrated into Figure 3 the corresponding XPS-diagrams are reported in the supporting information). EDAX relies on the limited penetration depth of electrons of relatively high kinetic energetic and yields the composition of the material within a region approximately 1 μm below the surface. Thus, it might contain information due to the shell and due to the core of the microspheres. XPS on the other hand is based on the limited escape depth of electrons of relatively low kinetic energy and reveals information on the topmost few angstroms of the surface. Thus, it is significantly influenced by surface oxidation and adsorption of organic molecules or ions. Both methods reveal the presence of those metals that were present in the plating bath, the absence of the metals not present in the plating bath, and the presence of phosphorus. Besides the elements that are expected to comprise the coating, both methods reveal significant amounts of additional elements, most notably carbon, oxygen, and aluminum. The aluminum signal is due to the sample holder. The carbon signal is due to the polymeric core, due to organic compounds absorbed from solution, and (in case of EDAX) due to the carbon layer applied to the top to prevent surface charging. The oxygen might indicate partial oxidation of the metals after synthesis. The most striking difference between the two methods is that XPS seems to reveal a significantly higher content of the lighter elements such as carbon and oxygen and of phosphorus than EDAX. Since XPS is sensitive to the topmost layers at the surface, we conclude that these elements are enriched at the surface of the coatings of the microsphere, partially due to the formation of an oxide layer on the surface and partially due to the adsorption of corresponding compounds from solution. The results of EDAX are less influenced by the topmost layer and thus more accurately represent the composition of the metal coating. According to EDAX analysis the ratio of phosphorus to metal is in all samples significantly below the ratios of the corresponding ions in the plating solutions but within the range already published in the literature. In the case of alloys that include Fe (CoFeP and NiFeP), we also observe that the Fe content is significantly lower than the ratio of Fe ions to the other metal ions in the plating bath. Even if present only as a minority component, the included iron is known to enhance the magnetic properties of the coated alloy.[23]

To compare the magnetic properties, we show in Figure 3 the magnetization curve of all the coated microspheres. From these curves it is clear that the particles' saturation magnetization (M_s) changes with the deposited alloy. We summarize all the calculated magnetic characteristics in Table 3 and compare them to the literature values of the pure Ni and Co. First we observe that all the M_s values are 10 times or more lower than the values of the pure metals. This is mainly due to the co-deposition of

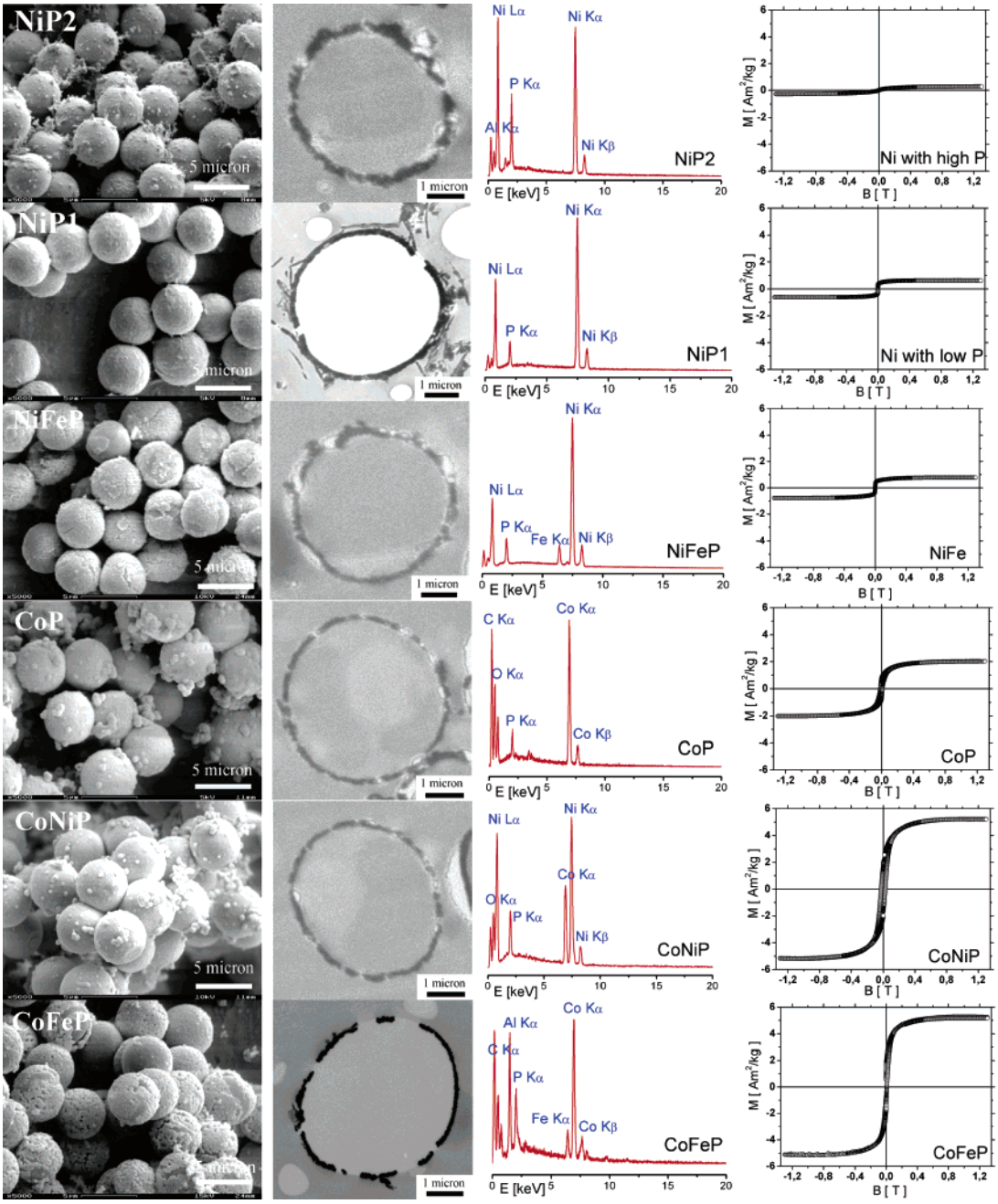

Figure 3. Characterization of PMMA particles coated with various plating procedures (see Table 1). From top to bottom row: NiP2 (Ni with high P content), NiP1 (Ni with low P content), NiFeP, CoP, CoNiP, CoFeP; from left to right: SEM, TEM, EDAX, magnetization loop of each of the samples.

the phosphorus and other non magnetic material (impurities) during the plating process. The microspheres coated with CoFeP and CoNiP have the highest M_s value, while the microspheres coated with a nickel-based alloy have the lowest value. This result is not surprising if one considers the fact that the saturation magnetization of Ni-based alloys must be lower than that for Co-based alloys for the same Co and Ni content.[24] Then, confirming our results is also the fact that the CoP alloy presents a lower M_s value compared to the CoFeP and CoNiP values.[17d] The M_s values of the microspheres depend also on the amount of phosphorus in the plated alloy. This is evident especially in the comparison between the alloys NiP1 and NiP2. The second has significantly higher phosphorus content and as a consequence a lower value of the saturation magnetization. To further enhance the magnetic properties of the microsphere, one might thus try to decrease the phosphorus content. The CoNiP alloy produced here still has a phosphorus content of ~8%; we expect that a modified formulation of the corresponding bath (Table 1) can give rise to particles with less phosphorus content and thus higher M_s. Equally, increasing the amount of Fe in the Ni-based alloys, can further increase the magnetic properties of the NiFeP and CoFeP alloys.[20,21] However, changing the composition of the bath can affect strongly the stability of the plating, and as a consequence, anomalous deposition, bath decomposition, or even nonplating of the microspheres can occur. We finally conclude that the plating baths used here are the best compromise between high M_s and adhesion of the plating to the spheres.

The magnetization curve of Figure 3 gives a first comparison between the magnetic properties of the coated microspheres.

TABLE 2: Composition of the Different Coated Microspheres Measured via EDAX and XPS Analysis[a]

	Coatings					
	NiP1	NiP2	NiFeP	CoP	CoNiP	CoFeP
			% At (EDAX)			
Ni	87.99	63.58	80.81		45.20	
Co				69.02	21.97	36.28
Fe			3.85			3.68
P	2.45	9.57	4.30	4.12	7.98	4,17
Al	5.89	0.76	2.31			22.80
O	3.67	9.02	8.37	8.03	24.85	33.07
C		17.07		18.83		
			Atomic Ratio			
Ni:Co:Fe:P	97:0:0:3	87:0:0:13	91:0:4:5	0:94:0:6	60:29:0:11	0:82:8:10
			% At (XPS)			
Ni	20.1	10.8	8.3		2.6	
Co				6.1	3.0	7.9
Fe			0.1			1.2
P	1.4	5.6	3.2	4.4	1.6	2.4
Al						
O	44.0	34.8	31.0	32.8	37.5	34.2
C	34.4	48.8	57.2	56.7	55.3	54.3
Na	<0.01					
K	0.01		<0.01	<0.01	<0.01	
			Atomic Ratio			
Ni:Co:Fe:P	94:0:0:6	66:0:0:34	72:0:1:27	0:58:0:42	36:42:0:22	0:69:10:21
			%At P/atomic ratios according to ref 17			
Ni, Co, Fe, P	1−2% P[17a]	>10% P[17a]	2−1%P[17b]	4% P[17c]	70:21:0:8[17d]	2−1% At[17d]

[a] The last row shows the molar ratio of the corresponding compounds present in the plating bath.

TABLE 3: Magnetic Properties for the Coated Microspheres and Literature Values for the Pure Metals[a]

	coated microspheres			bulk metals	
	M_s (Am^2/kg)	H_c (mT)	m (μ_B)		M_s (A m^2/kg)
NiP1	0.61	0.94		Ni	55.0[23]
NiP2	0.28	0	1.83	Ni	55.0[23]
NiFeP	0.73	0.68			
CoP	2.02	14.0		Co	167.0[23]
CoNiP	5.22	26.2			
CoFeP	5.25	3.2			

[a] M_s, saturation magnetization; H_c, coercive field, m: to the magnetic moment obtained from Langevin fit.

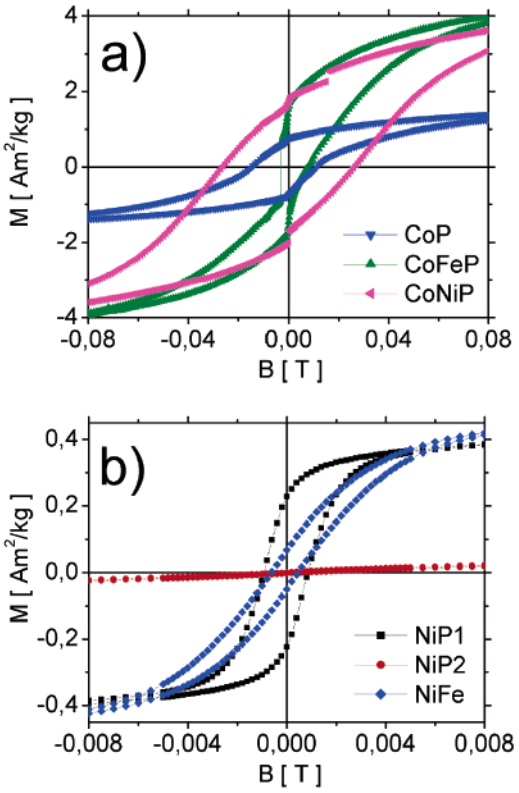

Figure 4. (a) Enlargement of the central parts of the magnetization loops of the microspheres coated with cobalt alloys (CoP, CoNiP, and CoFeP) taken from −0.08 T to 0.08 T. (b) Enlargement of the magnetization loops of the microspheres coated with nickel alloys (NiP1, NiP2 and NiFeP) taken from −0.008 T to 0.008 T.

To compare other properties, such as the coercivity, we report in Figure 4 two other diagrams. Figure 4a is an enlargement of the central part of the magnetization curve of all the microspheres coated with a cobalt-based alloy (CoP, CoNiP, CoFeP), while the second diagram reports also an enlargement of the hysteresis loop of all the coated microspheres with a nickel-based alloy (NiP1, NiP2, and NiFeP). The corresponding values of the calculated coercivity (H_c) are included in Table 3. The main differences between the reported curves is the slight or stronger ferromagnetic behavior presented by the particles. We observe that all the particles that have cobalt in the deposit show a large coercivity and a ferromagnetic character (first graph) while the others, (also the NiFe alloy, filled diamonds) present only a weak ferromagnetism or even a pure paramagnetic behavior (note the different scaling of the ordinate in Figures 4a and 4b).

This difference in the magnetic properties can be explained by the more crystalline structure of the microsphere coated with a cobalt alloy. From the broad peaks of the X-ray diffractogram one can conclude that the microspheres coated with nickel or Ni−Fe (∼4% Fe) have an amorphous nature with poor crystallinity (the XRD patterns for all particles are in the Supporting Information). This amorphous nature can be related to the heat treatment of the particles after plating. It has been reported that for electroless deposited nickel[21] a crystalline phase (Ni_3P) starts to appear above 300 °C of annealing. In our case, an annealing temperature of less than 150° was used due to the low softening temperature of the PMMA core. For the

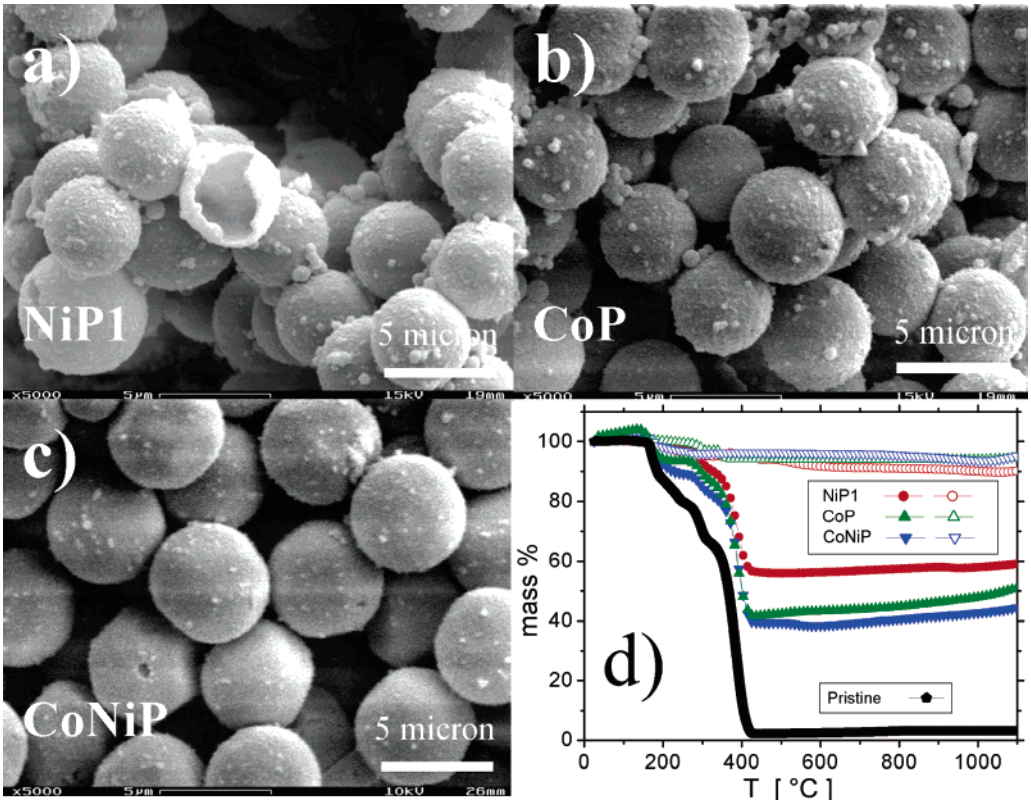

Figure 5. SEM pictures of hollow microspheres obtained by dissolving the polymer core: (a) NiP1, (b) CoP, (c) CoNiP, (d) thermogravimetric analysis of the hollow samples (hollow symbols) and of the plated spheres before dissolution (filled symbols) the colors are red for NiP1, green for CoP, and blue for CoNiP.

microspheres plated with a cobalt-based alloy, some Bragg reflections can be detected referring to the hcp cobalt or bcc Co−Fe. On the other hand, as mentioned in ref 17d, the Co−Fe phase is more difficult to observe with XRD due to the very low intensities of superstructural peaks.

The amorphous nature of the nickel for the particles coated with NiP1, NiP2, and NiFeP can also explain the fact that these microspheres present roughly the same M_s. The particles coated with Co, depending on the composition of the alloy, present a more dramatic variation in the M_s as well as in the coercivity. The phosphorus content in the deposit affects the magnetic characteristics of the nickel-coated particles more strongly than those of the cobalt-coated microspheres. While the NiP1- and NiFeP-coated particles present small coercivity for low field, the NiP2 particles have a paramagnetic behavior (see Figure 4b and Table 3). [Due to the paramagnetic behavior of the NiP2 sample we calculate the magnetic moment by fitting the magnetization loop with a Langevin function (see experimental section) and report the obtained value in Table 3.]

In addition to the above-mentioned results, we found that it was possible to remove the polymer core of the coated microspheres by dispersing them in a solvent for the core (toluene). Figure 5 shows three SEM images of such hollow metallic shells made by NiP1 (5a), CoP (5b), and CoNiP (5c) alloys. Although some broken shells or cracks are present (especially for the NiP1), these images show that overall uniform hollow metallic spheres were obtained from this procedure. To convince ourselves that almost all polymer material was dissolved, we subjected the spheres to TGA analysis. In Figure 5d we report the thermogravimetric analysis of these hollow particles (hollow symbols, circles for NiP1, upward pointing triangles for CoP, downward pointing triangles for NiCoP) together with the corresponding coated microspheres whose core was not dissolved (filled symbols) and the pristine particles before coating (black pentagons). The pristine particles decompose completely if heated to 400 °C. In case of the coated particles, heating induces weight loss of more than 40% due to the depolymerization of the polymeric core at 400 °C. This significant weight loss almost completely disappears if the core of the particles was dissolved with toluene, indicating that this washing procedure removed more than 90% of the polymer material.

Hollow metallic spheres, especially if made by different magnetic alloys, can find various applications based either on their magnetic properties (high saturation) or on their corrosion resistance, and strength at elevated temperatures (especially referred in this case for the CoP and CoNiP). Moreover, the nonconductive core of the metal-coated microspheres give a slight diamagnetic contribution to the total magnetic properties. Dissolving the core eliminates this effect, giving the pure magnetic answer of the alloy.

IV. Conclusion

In conclusion, we have successfully prepared and characterized various composite particles made by a poly(methyl methacrylate) core and various metallic shells (NiP, NiFeP, CoP, CoNiP, CoFeP). These coated microspheres were obtained using a combination of dispersion polymerization and electroless plating. The main advantage of this method is the fact that it is possible to precisely tailor the size of the deposited metal shell as well as the nature of the constituent metal. Consequently, microspheres with a broad variation of their magnetic properties − from ferromagnetic to even paramagnetic − were obtained. Finally dissolving the polymer core, uniform hollow metallic spheres made by nickel, cobalt, or nickel−cobalt alloy are easily obtained.

Acknowledgment. The support by K. Landfester (University of Ulm) is greatly appreciated. We especially thank Senthilnathan Mohanan for the VSM measurements, Jun Cai for the XPS analysis, Paul Walter for the use of the SEM and TEM, and Marlies Fritz for the TGA analysis. This work was supported by the Deutsche Forschungsgemeinschaft (SFB 569, SPP1052).

Supporting Information Available: Figures showing a SEM image of PMMA particles and a diagram of metal thickness, XRD pattern, and XPS spectra of the coated microspheres. This material is available free of charge via the Internet at http://pubs.acs.org.

References and Notes

(1) Pusey, P.; van Megen, W. *Nature* **1986**, *320*, 340. Davis, K. E.; Russel, W. B.; Glantschnig, W. J. *Science* **1989**, *245*, 507. Clark, N. A.; Hurd, A. J.; Ackerson, B. J. *Nature* **1979**, *281*, 57. Pieranski, P. *Contemp. Phys.* **1983**, *24*, 25. Van Blaaderen**,** A. *Science* **2003**, *301*, 470.

(2) Wang, N.; Butler, J. P.; Ingber, D. E. *Science* **1993**, *260*, 1124. Maniotis, A. J.; Chen, C. S.; Ingber, D. E. *Proc. Natl. Acad. Sci. U.S.A.* **1997**, *94*, 849.

(3) Nadal, F.; Argoul, F.; Hanusse, P.; Pouligny, B.; Ajdari, A. *Phys. Rev. E* **2002**, *65*, 061409-1. Aveyard, R.; Binks, B. P.; Clint, J. H.; Fletcher, P. D. I.; Horozov, T. S.; Neumann, B.; Paunov, V. N.; Annesley, J.; Botchway, S. W.; Nees, D.; Parker, A. W.; Ward, A. D.; Burgess, A. N. *Phys. Rev. Lett.* **2002**, *88*, 246102−1.

(4) Smith, S. B.; Finzi, L.; Bustamante, C. *Science* **1992**, *258*, 1122. Hosu, B. G.; Jakab, K.; Banki, P.; Toth, F. I.; Forgacs, G. *Rev. Sci. Instrum.* **2003**, *74*, 4158. Wirtz, D. *Phys. Rev. Lett.* **1995**, *75*, 2436.

(5) Crocker, J. C.; Grier, D. G. *J. Colloid Interface Sci.* **1996**, *179*, 298. Habdas, P.; Weeks, E. R. *Curr. Opin. Colloid Interface Sci.* **2002**, *7*, 196.

(6) Kim, D. K.; Zhang, Y.; Voit, W.; Rao, K. V.; Muhammed, M. *J. Magn. Magn. Mater.* **2001**, *225*, 30. Xu, X.; Friedman, G.; Humfeld, K. D.; Majetich, S. A.; Asher, S. A. *Chem. Mater.* **2002**, *14*, 1249. Kim, D. K.; Mikhaylova, M.; Zhang, Y.; Muhammed, M. *Chem. Mater.* **2003**, *15*, 1617.

(7) *Colloidal Polymers: Synthesis and Characterization*; Surfactant Science Series; Elaissari, A., Ed.; Marcel Dekker: New York, **2003**; Vol. 115, Chapter 11.

(8) Bizdoaca, E. L.; Spasova, M.; Farle, M.; Hilgendorff, M.; Liz-Marzan, L. M.; Caruso, F. *J. Vac. Sci. Technol.* **2003**, *21*, 1515. Pol, V. G.; Grisaru, H.; Gedanken, A. *Langmuir* **2005**, *21*, 3635. Imhof, A. *Langmuir* **2001**, *17*, 3579.

(9) Guo, H.-xia; Zhao, X.-peng; Ning, G.-hui; Liu, G.-qi *Langmuir* **2003**, *19*, 4884. Xu, X.; Asher, S. A. *J. Am. Chem. Soc.* **2004**, *126*, 7940. Sertchook, H.; Avnir, D. *Chem. Mater.* **2003**, *15*, 1690.

(10) Philipse, A. P.; van Bruggen, M. P. B.; Pathmamanoharan, C. *Langmuir* **1994**, *10*, 92.

(11) Velikov, K. P.; van Blaaderen, A. *Langmuir* **2001**, *17*, 4779. Averitt, R. D.; Sarkar, D.; Halas, N. J. *Phys. Rev. Lett.* **1997**, *78*, 4217.

(12) Giersig, M.; Ung, T.; Liz-Marzan, L. M.; Mulvaney, P. *Adv. Mater.* **1997**, *9*, 570.

(13) Wang, Y.; Wang, Y.; Feng, L. *J. Appl. Polym. Sci.* **1996**, *64*, 1843.

(14) Guo, H.-xia; Zhao, X.-peng; Guo, H.-lin; Zhao, Q. *Langmuir* **2003**, *19*, 9799.

(15) Park, J.-Gyu; Kim, J.-Woong; Oh, S.-Geun; Suh, K.-Do *J. Appl. Polym. Sci.* **2003**, *87*, 420.

(16) Tseng, C. M.; Lu, Y. Y.; El-Aasser, M. S.; Vanderhoff, J. W. *J. Polym. Sci., Part A: Polym. Chem.* **1986**, *24*, 2995. Shen, S.; Sudol, E. D.; El-Aasser, M. S. *J. Polym. Sci., Part A: Polym. Chem.* **1993**, *31*, 1393.

(17) (a) Mallory, G. O.; Hajdu, J. B. *Electroless Plating*; American Press: Cambridge, Great Britain, 1989; Chapter 1. (b) DePew, J. R. *J. Electrochem. Soc.* **1973**, *120*, 1187. (c) Homma, T.; Suzuki, M.; Osaka, T. *J. Electrochem. Soc.* **1998**, *145*, 134. (d) Zeng, Q.; Zhang, Y.; Bonder, M. J.; Hadjipanayis, G. C. *J. Appl. Phys.* **2003**, *93*, 6498.

(18) ImageJ is a freeware software available from the web at: <http://rsb.info.nih.gov/ij/>.

(19) Sard, R. *J. Electrochem. Soc.* **1970**, *117*, 864. Cohen, R. L.; D'Amico, J. F.; West, K. W. *J. Electrochem. Soc.* **1971**, *118*, 2042. Chow, S. L.; Hedgecock, N. E.; Schlesinger, M.; Rezek, J. *J. Electrochem. Soc.* **1972**, *119*, 1013.

(20) *Modern Electroplating*, 4th ed.; John Wiley: New York, 2000; Chapter 18, p 671.

(21) Lin, K.-L.; Lai, P.-J. *J. Electrochem. Soc.* **1989**, *136*, 3803.

(22) See for NiFe: Takai, M.; Kageyama, K.; Takefusa, S.; Nakamura, A.; Osaka, T. *IEICE Trans. Electron.* **1995**, *E78-C*, 1530; for CoFe: Yokoshima, T.; Nakamura, S.; Kaneko, D.; Osaka, T.; Takefusa, S.; Tanaka, A. *J. Electrochem. Soc.* **2002**, *149*, C375; and for CoNiP: Murthy, S. K.; Vemagiri, J. K.; Gunasekaran, R. A.; Coane, P.; Varahramyan, K. *J. Electrochem. Soc.* **2004**, *151*, C1.

(23) Cullity, B. D. *Introduction to Magnetic Materials*; Addison-Wesley: MA, 1972; Chapters 1−4.

(24) Myung, N. V.; Park, D.-Y.; Yoo, B.-Y.; Sumodjo, P. T. A. *J. Magn. Magn. Mater.* **2003**, *265*, 189.